

OBSERVATIONAL SIGNATURES OF X-RAY IRRADIATED ACCRETION DISKS

C. DONE¹ & S. NAYAKSHIN^{2,3}

¹ Department of Physics, University of Durham, South Road, Durham, DH1 3LE, England; chris.done@durham.ac.uk
² Laboratory for High Energy Astrophysics, NASA/Goddard Space Flight Center, Greenbelt, MD20771, USA;
 serg@milkyway.gsfc.nasa.gov

Draft version November 14, 2018

ABSTRACT

Reflection of X-rays from cool material around a black hole is one of the few observational diagnostics of the accretion flow geometry. Models of this reflected spectrum generally assume that the accretion disk can be characterized by material in a single ionization state. However, several authors have recently stressed the importance of the classic ionization instability for X-ray irradiated gas in hydrostatic balance. This instability leads to a *discontinuous* transition in the vertical structure of the disk, resulting in a hot ionized skin above much cooler material. If the Compton temperature of the skin is high then even iron is completely ionized, and the skin does not produce any spectral features. These new models, where the ionization structure of the disk is calculated self-consistently, require an excessive amount of computing power and so are difficult to use in directly fitting observed X-ray spectra. Instead, we invert the problem by simulating X-ray spectra produced by the new reflection models, and then fit these with the old, single zone reflection models, to assess the extent to which the derived accretion geometry depends on the reflection model used. We find that the single zone ionization models can severely underestimate the covering fraction of the “cold” material as seen from the X-ray source if the optical depth in the ionized skin is of order unity, and that this can produce an apparent correlation between the covering fraction and the X-ray spectral index similar in nature to that reported by Zdziarski, Lubinski and Smith (1999).

Subject headings: accretion, accretion disks — radiative transfer — line: formation — X-rays: general — radiation mechanisms: non-thermal

1. INTRODUCTION

Calculations of the reflected spectrum expected from X-ray illumination of an accretion disk around a black hole are extremely important. The reflected continuum and especially its associated iron K α fluorescence line (see e.g. Basko, Sunyaev & Titarchuk 1974; Lightman & White 1988; George & Fabian 1991; Matt, Perola & Piro 1991) are perhaps the only spectral features expected from optically thick material in the vicinity of a black hole, so can be used to test theoretical models of accretion in strong gravity (Fabian et al. 1989, Dabrowski et al. 1997).

This is especially relevant since there is much current debate on the structure of the accretion flow. The “standard” accretion disk models of Shakura & Sunyaev (1973: hereafter SS) are clearly incomplete. They can produce UV and soft X-ray emission, but not the hard X-ray power law out to 200 keV. This is observed to carry a significant fraction of the luminosity in Active Galactic Nuclei (AGN) and Galactic Black Hole Candidates (GBHC) in their low/hard state. Something other than the SS disk is required. The two current candidates are either magnetic reconnection regions above the accretion disk, or that some part of the accretion flow is in an alternative (non-disk) configuration.

The idea of magnetically powered active regions above a disk (e.g. Galeev, Rosner & Vaiana 1979) gained considerable plausibility from the recent discovery that the accretion disk viscosity is driven by a magnetic dynamo (Balbus & Hawley 1991). Buoyancy could then make the magnetic loops rise to the top of the disk, where the optical depth is low so that the energy released in reconnection cannot thermalize (e.g. di Matteo 1998). Such active regions could give the hard X-ray spectra which are

seen from AGN and Galactic Black Hole Candidates (Haardt, Maraschi & Ghisellini 1994; Stern et al. 1995; Beloborodov 1999a,b). Spectral transitions between the low/hard state and the high/soft state in GBHC might then be associated with the disk becoming radiation pressure dominated. This occurs at a few percent of the Eddington accretion rate, roughly as observed in Cyg X-1 and other GBHCs. Perhaps magnetic buoyancy transfers more energy out of the disk and into a corona in gas dominated disks than in radiation pressure dominated ones (Nayakshin 1999a). Current (though still incomplete) MHD simulations do show strong magnetic fields in the low density regions above and below the disk (Hawley 2000), although they do not yet carry enough power to reproduce the observed low/hard state (Miller & Stone 2000).

The idea of an alternative accretion flow became a serious contender with the rediscovery of another stable solution of the accretion flow equations for mass accretion rates below ~ 10 per cent of Eddington. The standard SS disk model derives the accretion flow structure in the limit where the gravitational potential energy is radiated locally. This assumption is relaxed in the Advection Dominated Accretion Flow (ADAF) models, so that the energy can be transported radially (adverted), as well as radiated locally. There are two key (and currently uncheckable) assumptions underlying this: firstly that the viscosity mechanism gives the accretion energy to the protons (as opposed to both protons and electrons) and secondly that the protons transfer this energy to the electrons only via (rather slow) electron-ion (Coulomb) collisions. This gives an accretion flow which is optically thin, geometrically thick and *hot*, with typical electron temperatures of order 200 keV as observed (e.g. Narayan & Yi 1995). This model provides a rather natural explanation for the low/hard to high/soft spectral state transitions in GBHCs, as

ADAFs cannot exist at high mass accretion rates. The electron-ion collision rate increases with the density of the flow, and so above a mass accretion rate of ~ 10 per cent of Eddington (as long as the disk viscosity parameter $\alpha \sim 0.2$; Esin, McClintock & Narayan 1997, Quataert & Narayan 1999) the electrons can drain most of the energy from the protons. Advection is then unimportant as the electrons radiate the gravitational energy released locally, and the flow collapses into an SS disk.

In the one model, there is an optically thick disk extending down to the last stable orbit at 3 Schwarzschild radii. In the alternative, the inner disk is truncated, with the optically thick, cool flow replaced by an optically thin, X-ray hot plasma. The reflected spectrum gives an observational test between these two scenarios. Firstly the amount of reflection should be different. A disk with active regions above it should subtend a solid angle of roughly 2π , whereas a truncated disk with the X-ray hot plasma filling the “hole” in the disk will subtend a rather smaller solid angle. Secondly, for the SS disk there is material down to the last stable orbit. Reflection features from the inner disk should then be strongly smeared and skewed by the combination of special and general relativistic effects expected in the vicinity of a black hole (Fabian et al. 1989). This material is not present in the truncated disk models, so they should have narrower lines.

The seminal ASCA observation of the AGN MCG-6-30-15 showed that the line is so broad that accretion disk models require that the material extends down to *at least* the last stable orbit in a Schwarzschild metric (Tanaka et al. 1995), and that it subtends a solid angle of $\sim 2\pi$ with respect to the X-ray source (Lee et al 1999). This very clear cut result gives strong support for the existence of an SS accretion disk, although other interpretations in terms of optically thick, highly ionized cloudlets close to the black hole rather than a smooth disk flow may be possible (Karas et al 2000).

However, the line and reflected continuum seen from the GBHCs in their low/hard state (where the X-ray continuum bears a remarkable similarity to that from Seyfert 1 type AGN) are *not* the same as that seen in MCG-6-30-15. The GBHC have reflection amplitudes which are rather less than expected for a hard X-ray source above a disk (e.g. Gierlinski et al. 1997; Done & Źycki 1999). The iron line does not generally show the extreme smearing associated with material within 5 Schwarzschild radii, although there is detectable broadening of the line showing that there is cool, optically thick material within $\sim 10 - 20$ Schwarzschild radii (Źycki, Done & Smith 1997; 1998; 1999; Done & Źycki 1999). It is also emerging that while some Seyfert 1 AGN do have extremely broadened iron lines like MCG-6-30-15 (e.g. NGC 3516; Nandra et al. 1999), others look more like the GBHC in not having the extreme skewed lines expected from the very inner disk (e.g. IC4329a; Done, Madejski & Źycki 2000), and that many do not show reflection subtending the expected 2π solid angle (Smith & Done 1996; Zdziarski, Lubiński & Smith 1999).

Can this be interpreted as a strong evidence that the accretion flow is not always given by an optically thick disk? Such a conclusion is plainly consistent with the data. Perhaps the objects with extreme line profiles have high mass accretion rates, where the ADAF’s cannot exist. Perhaps these are the analogue of the GBHC in their high/soft state (Done & Źycki 1999; Zdziarski et al. 1999). Alternatively, Ross, Fabian & Young (1999) argue that the lack of strong reflection and extreme relativistic smearing does not necessarily imply the absence of an inner disk, be-

cause the reflection signature from the disk can be masked by complex ionization effects. For completely ionized gas, there is no photo-electric absorption opacity left, so the reflected spectrum is simply due to electron scattering in the disk atmosphere. There is then no characteristic iron line or edge feature from the inner disk, so the extreme relativistically smeared components of the line are not present.

However, illumination of a disk with density given by the SS models results in a power law distribution of ionization state with radius (Ross & Fabian 1993; Matt, Fabian & Ross 1993). This does not fit the data when the inner radii have a high enough ionization to mask their reflected signature (Źycki et al., 1998; 1999; Done & Źycki 1999). The key problem is that the observed reflected spectra from the low/hard state GBHC are relatively neutral (Źycki et al., 1998; 1999; Done & Źycki 1999). Yet if the inner disk is extremely ionized, then there should exist a transition region in which the disk is cool enough for H- and He-like iron to exist, before getting to the low-to-moderate ionization material at larger radii. These species give an unmistakable reflected signature, with very strong, highly ionized line and edge features (Lightman & White 1988; Ross & Fabian 1993; Matt, Fabian & Ross 1993ab; Źycki et al., 1994; Matt, Fabian & Ross 1996; Ross, Fabian & Brandt 1996), which are simply not present in the data. This leads to the conclusion that either the disk really does subtend a small solid angle to the X-ray source, or that its ionization state drops dramatically (as a step function rather than a power law) from extreme ionization to relatively neutral (Done & Źycki 1999), or/and that the X-ray source does not illuminate the inner disk (e.g. through the anisotropic illumination pattern resulting from trans-relativistic outflow from magnetic reconnection: Beloborodov 1999a,b).

This argument is based on reflection models which neglect the energy change which can result from Compton scattering below $\sim 10 - 15$ keV, and assume that the ionization state is constant with depth in the material. In practice, at high ionization states the electron temperature in the disk can be high enough to cause appreciable Comptonization smearing of the resulting reflected spectrum and line. Also, there is vertical ionization structure of the illuminated material, the details of which depend on the vertical density structure of the disk (Ross & Fabian 1993; Źycki et al 1994; Matt, Fabian & Ross 1996; Ross, Fabian & Young 1999). Ross, Fabian & Young (1999) argue that these effects alone are sufficient to hide the otherwise unmistakable signature of highly ionized reflection from H- and He-like iron, but this has yet to be tested against real data.

However, all these works use an *assumed* vertical density structure. This is a very crude simplification, which can severely misrepresent the reflection signature from the disk (Nayakshin 1999b; Ross, Fabian & Young 1999). X-ray illumination *changes* the density structure of the material. Material at the top of the disk is heated by the illumination, and so can expand, lowering its density. Deeper into the disk there is less X-ray heating, so the material is cooler, and hence denser. The self-consistent density structure is especially important as there is a thermal ionization instability which affects X-ray illuminated material in pressure balance (Field 1965; Krolik, McKee & Tarter 1981; Kallman & White 1989; Ko & Kallman 1994; Różańska & Czerny 1996; Różańska 1999; Nayakshin, Kazanas & Kallman 2000, hereafter NKK). This can result in the ionization state of the material changing very rapidly, with

a highly ionized skin forming on top of a mainly neutral disk. If the ionization state of the skin is high enough to completely strip iron then it is almost completely reflective, and forms no spectral features. The observed reflected signature is then dominated by photons reflected from deeper in the disk, where the material is mainly neutral. Although the material is still expected to be less ionized at larger radii, the meaning of less ionized is very different from that in the constant density models – the skin remains completely ionized with a negligible amount of H- and He-like iron, but its Thomson depth decreases with radius (see Nayakshin 2000). The instability gives a physical mechanism for a discontinuous transition in ionization state, as required by the data.

The small observed solid angle subtended by the disk could then be an artifact of fitting single zone ionization models to data from systems with more complex ionization structure. Ideally we would want to reanalyze the data, fitting these X-ray illuminated disk reflection models to derive the solid angle subtended by the reflecting material. If these models give a worse fit to the data than the single ionization models, or if they give a derived solid angle of the reflector which is much less than 2π then the “hole in the disk” geometry inferred from the single zone ionization models is still favored. If instead the complex ionization reflector models are a better fit to the data and give a solid angle which is compatible with 2π then the SS disk with magnetic coronal X-ray source is probably correct, and the previous results which ruled out this geometry are a model dependent interpretation of the data.

However, direct data fitting is prohibitively CPU intensive. The models require simultaneous computation of the hydrostatic, ionization and energy balance for the illuminated gas plus optically thick radiation transfer and relativistic effects to determine the reflected spectrum. A single model calculation requires ≈ 1 day of CPU on a 500 MHz workstation. Given this, we have chosen to tackle the inverse problem. Instead of fitting real data with the complex ionization reflector code, we use the complex ionization reflector code to synthesize a spectrum with the same signal-to-noise and spectral resolution as given from typical *GINGA* observations of the low/hard state spectra from Galactic Black Hole Candidates. We then fit this model spectrum with the standard (and computationally very fast) single zone ionization reflection models which are widely used in X-ray spectral analysis. We can then quantify the effect of using the single zone ionization reflection models to describe a more complex ionization disk structure.

We show that the resulting spectra from a complex ionization structure disk subtending a solid angle of 2π are well fit over the 2–20 keV range by the single zone reflection models, but that the presence of the ionized skin leads to an underestimate of the covering fraction of the reflector. The SS disk models then cannot be ruled out by the fact that single zone ionization reflector models derive a solid angle of $\ll 2\pi$. The complex ionization structure disks can also produce a correlation between the amount of reflection as measured by the single zone ionization models and the spectral index (as observed e.g. by Zdziarski et al., 1999) *without* changing the solid angle subtended by the disk. We end by discussing how we can observationally distinguish between the truncated disk models and complex ionization structure.

2. THE SPECTRAL MODEL

We use the code of NKK to calculate the reflected spectrum from a X-ray illuminated disk model. This code

putes the vertical structure assuming hydrostatic equilibrium, solving simultaneously for the density, ionization structure and energy balance of the illuminated gas, as well as doing the radiative transfer for the continuum and emission lines. Locally, the amount of photo-ionization can be described by the parameter, $\Xi = F_x/(cP_{gas})$, which is the ratio of the illuminating radiation pressure (F_x/c , where F_x is the illuminating hard X-ray flux) to the gas pressure ($P_{gas} = 2.3n_H kT$ acting outwards, where n_H is the hydrogen density and T is the temperature). This relates to the more usual density ionization parameter $\xi = 4\pi F_x/n_H$ by $\xi = 2.3\Xi kT/4\pi c$.

As results of NKK show, the vertical density structure of the illuminated layer is rather complex (see also Nayakshin & Kallman 2000), as the gas in radiative equilibrium with the illuminating X-rays is subject to a thermal pressure ionization instability (Krolik, McKee & Tarter 1981). In the context of the given problem, the instability can be described as following. The X-ray heating clearly depends on height, with the material at the top of the layer being heated the most. Because the material is in pressure balance, the gas pressure is smallest at the top of the disk, so Ξ is at its maximum here. This corresponds to the uppermost stable branch of the ionization equilibrium S-curve (see Fig. 1 in NKK), with low density material which is highly or completely ionized. Atomic cooling is negligible so the temperature is a fraction of the local Compton temperature (see Krolik et al., 1981 and Nayakshin 2000a); Compton heating is balanced by bremsstrahlung and Compton cooling. Going deeper down into the disk, the X-ray heating decreases with optical depth to electron scattering, τ_h , and the gas pressure increases. Hence, both the temperature and ionization parameter Ξ decrease. However, there is then a turning point on the S-curve (point c in Fig. 1 of NKK). At this point the temperature and density is such that the rapidly increasing bremsstrahlung cooling causes the temperature to dramatically decrease. This pulls the gas pressure down, but hydrostatic equilibrium requires that the gas pressure must monotonically increase as a function of depth into the disk. The only way for the pressure to increase in a region with rapidly decreasing temperature is to rapidly increase the density, but this pushes up the cooling still further, and so decreases the temperature. Ionic and atomic species can now exist, so line transitions give a yet further increase in the cooling. Eventually this stabilizes onto the bottom part of the S curve, where the X-ray heating is balanced primarily by line cooling from low temperature, high density material. This results in an almost discontinuous transition from a highly ionized, hot and relatively tenuous skin to mainly neutral, cool and relatively dense material over a very small ($\Delta\tau_h \sim 10^{-3}$ – see Appendix in NKK) change in optical depth at $\Xi = \Xi^* \sim$ few.

The optical depth where this instability occurs plus the Compton temperature (which depends on the illuminating power law as well as the local thermal disk spectrum) are the main determinants of the resulting reflected spectrum. The majority of the reflected flux arises from the hot layer if its optical depth $\tau_h > 1$. The reflected spectrum then contains the imprints of the ionized material which can be either highly ionized (where iron is mainly He- or H-like), or extremely ionized (where even iron is completely stripped of bound electrons) depending on the equilibrium Compton temperature (Nayakshin & Kallman 2000). For smaller optical depths, $\tau_h < 1$, most of the reflection occurs in material below the ionization instability point, so the reflected spectrum contains the signatures of the cool material at low ionization states. NKK also find

sionless parameter A , which is essentially the ratio between the gravity force and that from the X-ray radiation pressure ($1.2n_H\sigma_t F_x/c$). Where gravity is dominant ($A \gg 1$) then the vertical disk structure is close to that of an un-illuminated disk (assumed here for simplicity to be the Gaussian density profile expected from a gas pressure dominated disk: Shakura & Sunyaev 1973) and the optical depth of the hot, ionized layer is very small. Conversely, where $A \ll 1$ then the illumination determines much of the vertical structure, and the optical depth of the hot layer is large. NKK give a simple analytic approximation to this hot layer optical depth of $\tau_h \sim (\Xi^* A)^{-1}$ (see also Kallman & White 1989; Nayakshin 2000 for more accurate analytical estimates of τ_h).

Given that the observations of flat spectrum AGN and low/hard state GBHC seem to show small but not negligible amounts of low to moderate ionization reflection, then the parameters which are most likely to reproduce this are $\tau_h \sim 1$, which corresponds to $A \sim 0.3$ for hard spectra. If the Compton temperature in the upper, ionized skin is high enough then the reflected spectrum from this will be featureless, and so not detected in X-ray spectral fitting. The observable reflection signature will then be given only by the material below the ionization instability point, where the incoming flux has been decreased by scattering in the hot layer. This reflected continuum then has to escape out through the hot layer, so scattering again reduces its amplitude and introduces some broadening to the reflected features.

A truly self-consistent model should uniquely determine the illuminating flux at the surface of the disk as a function of the system parameters (mass, radius and mass accretion rate through the disk). Since the X-ray energy generation mechanism for magnetic flares is not yet understood in detail then such a model is not yet available. Instead we *assume* a given X-ray illuminating flux in order to demonstrate the physical behavior of a disk atmosphere irradiated by magnetic flares. We calculate the angle averaged upward reflected spectra (corresponding to an inclination of $\sim 60^\circ$) resulting from a disk at $R = 10R_S$ ($R_S = 2GM/c^2$, the Schwarzschild radius), with an accretion rate of $\dot{m} = 10^{-3}\dot{m}_{Edd}$ onto a super-massive black hole of $10^8 M_\odot$. The large black hole mass means that we avoid disk photons potentially contributing to the observed bandpass. We assume a power law illuminating continuum with exponential cutoff at 200 keV. The illumination parameter is fixed at $A = 0.3$, and the resulting angle averaged upward reflected spectra (so corresponding to an inclination of $\sim 60^\circ$) are calculated for photon indices of $\Gamma = 1.5, 1.7, 1.9, 2.1, 2.3$ and 2.5 . We do not include any general or special relativistic shifts for simplicity. Figure 1 shows the reflected spectra (without the illuminating power law) and the gas temperature profiles for the 6 different values of Γ .

3. OVERALL 2–20 KEV SPECTRAL SHAPE

We simulate a 10ks observation with the GINGA X-ray satellite, using the `fakeit` command in XSPEC (Arnaud 1998), adding 0.5 per cent systematic errors to the results since it seems unlikely that any satellite will be calibrated to better than this limit. We compare these simulated spectra with the angle dependent reflection code of Magdziarz & Zdziarski (1995), with ion populations calculated as in Done et al. (1992), implemented in the `pexriv` model in XSPEC. This calculates the continuum reflection for an input spectrum which is a power law with exponential cutoff. It does not include the associated ionization instability, so it is not strictly valid for the

0.1 keV Gaussian line of free normalization, and energy (except that this latter is constrained to be between 5.5 and 7.5 keV, as expected for iron with some shifts allowed for Doppler and gravitational effects). We assume solar abundances (Morrison & McCammon 1983) and an inclination of 60° . We also include a free absorbing column in our fits so as to match as closely as possible the uncertainties which arise in fitting real data.

Figure 2 shows the spectral index and amount of reflection inferred from fitting the simulated datasets with the `pexriv` model, with full results given in Table 1. There is a clear correlation of the amount of reflection and its ionization state with spectral index. For hard spectra the ionization of the detected reflected spectrum is low, and the amount of reflection is much less than unity. This is because the Compton temperature of the upper layer of the disk is high, its ionization is extreme and it is Thomson thick ($\tau_h \simeq 1$, see Fig. 1). This produces a reflected spectrum which is mostly from electron scattering in the skin, which has few spectral features and cannot easily be identified as reflected flux. The ionization drops dramatically at the depth where the ionization instability sets in, so there is also a small reflected component from low ionization material which is fit by the `pexriv` model. However, this itself has to escape out through the skin, and so some fraction is Compton scattered, reducing the line and edge features from the low ionization reflected spectrum, but keeping its overall shape.

For steeper spectra the Compton temperature of the upper layers drops, so that its ionization is not so extreme, leading to strong spectral features from the ionized upper layer, plus the skin is actually thinner (see Fig. 1), and hence most of the reflected flux is easily identified. Figure 2 also shows the detected line equivalent width. It is generally low, but consistent with the theoretically expected equivalent width for the given ionization state (assuming that resonant trapping is not important) and spectral index, scaled by the observed solid angle (Życki & Czerny 1994; George & Fabian 1991).

The high energy cutoff is never detected (see Table 1), despite the fact that an exponential roll-over temperature at 200 keV gives a 10 per cent effect at 20 keV. This is probably due to the weak line and edge features compared to the Compton hump in the complex models due to Compton scattering of the low ionization reflected signature in the skin. Therefore, for a given reflected *continuum*, the models of NKK always have less of the absorption edge than the single ionization zone models (see also Ross, Fabian & Young 1999 who came to similar conclusions for exponential density profiles).

Hence, when using the single zone models, by fixing the depth of the photo-absorption edge (with the edge energy fixing the ionization state), one in fact picks a particular value for R already. This value is too small to reproduce the continuum reflection rise of our models shown in Fig. 1, but the fitting compensates for this by increasing the exponential cutoff energy. However, we caution that an exponential cutoff is much less sharp than the roll-over in a true Comptonized spectrum, so this aspect of the modeling need not be reproduced in detail by real illuminated disks.

All the fits are statistically very good, with $\chi^2 \leq 25$ for 22 degrees of freedom. However, there should be some observable features from these disk models with structured ionization which distinguish them from simple single ionization state models. Figure 3 shows the total spectrum and reprocessed components from the $\Gamma = 1.5$ flat spectrum simulation, to illustrate this in a more quantitative way.

TABLE 1

SIMULATED GINGA SPECTRA FROM THE ILLUMINATED DISK MODELS OF NAYAKSHIN ET AL., (2000) FIT TO SIMPLE REFLECTION MODELS (WITH ASSUMED SOLAR ABUNDANCES AND INCLINATION OF 60°). ERRORS ARE CALCULATED FOR $\Delta\chi^2 = 2.7$

Intrinsic Γ	Fit Γ	$E_{\text{cut}}^{\text{a}}$	Norm ^b	$\Omega/2\pi^{\text{c}}$	ξ^{d}	Line Energy ^e	Line Eqw (eV)	χ^2_{ν}
1.5	$1.57^{+0.01}_{-0.02}$	> 1100	2.3	$0.31^{+0.04}_{-0.05}$	$63^{+172}_{-62.9}$	$6.2^{+0.8}_{-0.7}$	11^{+12}_{-11}	12.9/22
1.7	$1.76^{+0.02}_{-0.01}$	> 1000	5.4	0.36 ± 0.05	$8.5^{+80}_{-8.4}$	$6.3^{+0.5}_{-0.6}$	18 ± 14	16.5/22
1.9	$1.97^{+0.01}_{-0.02}$	> 1000	7.2	0.47 ± 0.06	$20^{+80}_{-19.3}$	$6.3^{+0.3}_{-0.2}$	30^{+20}_{-15}	18.1/22
2.1	2.19 ± 0.02	> 1200	10.0	$0.63^{+0.07}_{-0.06}$	140^{+190}_{-85}	6.4 ± 0.2	45^{+16}_{-17}	25.2/22
2.3	2.39 ± 0.02	> 1200	13.2	$0.72^{+0.08}_{-0.07}$	300^{+490}_{-150}	6.5 ± 0.2	42^{+19}_{-18}	25.2/22
2.5	2.58 ± 0.02	> 800	17.1	0.8 ± 0.09	630^{+800}_{-320}	6.4 ± 0.2	38^{+18}_{-16}	10.9/22

^aExponential cutoff energy (keV)

^bNormalization at 1 keV

^cSolid angle subtended by the reprocessor with respect to the X-ray source.

^dIonization parameter of the reprocessor

^eLine energy (keV) constrained between 5 and 7 keV for stability of the fit

gether with the best fit model using the `pexriv` simple (single zone) ionization reflected spectrum. Plainly the absorbed power law and its reflected (`pexriv`) component give an excellent fit to the total spectrum derived from the complex ionization state models, but the individual components are not at all well modeled. The true reflected flux is dramatically underestimated and the derived “intrinsic” spectrum is somewhat steeper. These two together would give a rather steeper total spectrum, but this is compensated for by the lack of high energy cutoff in the fitted spectrum. With broad band data, extending significantly above 20 keV then there should be significant residuals from fitting true complex ionization spectra with the `pexriv` code.

Even in the 2–20 keV band it is plain that there is excess reflected flux at low energies in the stratified ionization model which is not matched by the single zone ionization state code. This excess is at the 10 per cent level, and should easily be detectable. We include a broad soft excess component in the fit to mimic this, using the `compst` (Sunyaev and Titarchuk 1980) model in XSPEC. This leads to a significant reduction in χ^2 for the flat spectra (see table 2). The resulting reduced χ^2 values are typically very much less than unity because the model is sometimes an adequate fit to the simulated data *without* systematic errors (photon counting errors are of the order of 0.05 per cent!). Error ranges are then derived from $\Delta\chi^2/\chi^2_{\nu} = F = 2.7$, rather than the standard $\Delta\chi^2 = 2.7$ which assumes that the fit has $\chi^2_{\nu} \sim 1$. Several of the parameters are tightly correlated, so error ranges on a single parameter are somewhat misleading.

Figure 4 shows the resulting fit to the simulated $\Gamma = 1.5$ spectrum. Comparison with Figure 3 shows that the broad soft excess component is used to describe the highly ionized reflected flux at low energies, while the fitted reflected flux is still dramatically underestimated.

4. DISCUSSION

4.1. Small covering fraction

The classic ionization instability can cause a dramatic transition in the vertical structure of an X-ray illuminated accretion disk, with an extremely ionized skin overlying low ionization material. With flat spectrum illumination the Compton temperature of the skin is high enough that even iron is completely stripped, so it only scatters the incident power law radiation and does not create any atomic features in the reflected spectrum (such as emission lines and photo-absorption edges). The only observable reflected signature then comes from the material below the ionization instability, which has low-to-moderate ionization. The instability suppresses any signature of H- and He-like iron, which was the key argument used by Done & Życki (1999) against substantial ionization of the disk. Where the optical depth in the ionized skin is ~ 1 then the observed reflected spectrum and line derived from single zone ionization models is suppressed by about a factor 3–4, as observed in the flattest AGN and GBHC. Thus, the geometry in which the disk covers half the sky as seen from the X-ray source (e.g., magnetic flares above a disk) *can* be consistent with the observed data because the reflected spectra computed with hydrostatic balance models *appear* to have a small reflection fraction when fitted with the current single-zone models. However, more detailed studies of this issue, with radial stratification of the skin properties, and with effects of possible X-ray induced evaporation (which is important for magnetic flares, see NKK) is needed to resolve the issue truly self-consistently.

We estimate that Thomson depth of the skin should be in the range of unity to few to explain spectra typical of hard state of GBHCs. At first glance, this seems to be a rather narrow range in parameter space, making the model appear contrived. However, the dependence of τ_h on F_x becomes very weak once $\tau_h \gtrsim 1$, because the incident X-rays are efficiently down-scattered in the skin. As discussed by Kallman & White

TABLE 2

SIMULATED GINGA SPECTRA FROM THE ILLUMINATED DISK MODELS OF NAYAKSHIN ET AL. (2000) FIT TO SIMPLE REFLECTION MODELS AND A SOFT EXCESS COMPONENT. ERRORS ARE CALCULATED FOR $\Delta\chi^2 = 2.7 \times \chi_\nu^2$

Intrinsic Γ	Fit Γ	Norm	kT	τ	Compt Norm	$\Omega/2\pi^a$	ξ^b	χ_ν^2
1.5	$1.37^{+0.09}_{-0.08}$	1.4	$1.9^{+0.6}_{-0.2}$	$15.5^{+1.5}_{-2.5}$	0.6	$0.12^{+0.13}_{-0.09}$	60^{+2000}_{-56}	1.00/19
1.7	1.55 ± 0.1	3.3	$1.9^{+1.3}_{-0.2}$	14 ± 4	1.6	$0.14^{+0.39}_{-0.14}$	$4^{+\infty}_{-4}$	3.85/19
1.9	$1.75^{+0.08}_{-0.11}$	4.2	$2.1^{+1.4}_{-0.3}$	$11.6^{+2.6}_{-2.7}$	2.6	$0.23^{+0.38}_{-0.11}$	50^{+930}_{-46}	4.05/19
2.1	$1.90^{+0.06}_{-0.04}$	5.4	$1.8^{+0.7}_{-0.3}$	11^{+1}_{-3}	4.0	$0.22^{+0.18}_{-0.08}$	900^{+3000}_{-700}	3.66/19
2.3	$2.12^{+0.06}_{-0.08}$	7.5	$1.5^{+0.6}_{-0.2}$	$11.5^{+1.3}_{-1.5}$	4.9	$0.2^{+0.16}_{-0.06}$	3000^{+16000}_{-1000}	5.36/19
2.5	2.40 ± 0.04	11.9	$1.3^{+0.5}_{-0.3}$	12 ± 3	3.7	0.37 ± 0.07	3000^{+3000}_{-1000}	2.50/19

^aSolid angle subtended by the reprocessor with respect to the X-ray source (assuming solar abundances and inclination of 60°)

^bIonization parameter of the reprocessor

(1989) and Nayakshin (2000a), it is then very difficult to produce $\tau_h \gtrsim \tau_* \sim$ a few even with arbitrarily large values of F_x . Therefore, the range of “acceptable” values of Thomson depths, $1 \lesssim \tau_h \lesssim$ few, may actually correspond to a change in the X-ray ionizing flux by several orders of magnitude, and hence the model may be quite robust in the parameter space.

4.2. Covering fraction – spectral index – ionization correlation

We find a strong apparent correlation between the inferred intrinsic spectral index and the amount of reflection and its ionization (see Fig. 2 and Table 1). The gas pressure at which the transition from the hot to the cold material occurs, P_t , scales with the Compton temperature as $P_t \propto T_1^{3/2}$ (see eq. 4 in Nayakshin 2000a). Therefore, the cold layer lies closer to the top of the skin for larger Γ for a given illuminating flux. In our numerical simulations the Thomson depth of the skin changes from $\tau_h \simeq 1.0$ for $\Gamma = 1.5$ to $\tau_h \simeq 0.2$ for $\Gamma = 2.5$ (see Fig. 1). The thicker the skin, the more it masks the cold material below it (e.g., see NKK), and so the correlation between Γ and $\Omega/2\pi$ that we found in this paper is to be expected.

The correlation of the inferred ionization state (ξ) with Γ comes about as a consequence of changes in τ_h and the actual ionization state of the skin with changes in the spectral index. In particular, when Γ increases, the Compton temperature, and hence the skin’s temperature, decrease (see Nayakshin & Kallman 2000 on this). For $\Gamma \gtrsim 2$, the skin is highly ionized, rather than extremely ionized, and so it produces strong features from H- and He-like iron. However, its optical depth is not very large for the parameters chosen in this paper (see Fig. 1). Hence, there is a substantial contribution to the reflected spectrum from the low to moderate ionization material under the ionized skin. The “observed” ionization state is a compromise between the optically thin, ionized skin and the low ionization material below, which then leads to the inferred correlation of ξ and Γ .

It is also interesting to note that a larger Thomson depth of the ionized skin leads to larger integrated X-ray albedo, a . The low- Γ models have a very large soft X-ray flux, while the high-

flux is $F_{\text{repr}} = (1 - a) F_x$. Thus, the thicker the ionized skin, the less reprocessed radiation will emerge, which means that Compton cooling of the magnetic active regions above the disk will be reduced. This is why Nayakshin (1999b) and Nayakshin & Dove (2000) find that larger values of τ_h lead to hotter coronae above the disk, i.e., smaller values of Γ if the optical depth of the corona is fixed. In other words, a complete self-consistent calculation, where Γ is not a fixed parameter, but it is rather found via balancing energy heating and cooling in the corona would produce *even stronger* apparent correlation between Γ and $\Omega/2\pi$ than the one we found here. These findings appear to be very relevant for the recently found correlations between Γ and $\Omega/2\pi$ for a sample of AGN and GBHCs, as well as for some individual sources (e.g., Zdziarski, et al. 1999).

Note also that the correlation between ξ and Γ inferred in our models suggest that sources with steeper X-ray spectra should produce spectra that *appear* to be more ionized than those of sources with harder spectra. This statement is only correct in the statistical sense, though. Namely, if for every Γ there is a range of illumination parameters A , then at a given A , there will be a correlation of ξ and Γ similar to that shown in Fig. 1. Folded with a range of A for every Γ , one still expects to see a similar correlation, probably somewhat weaker than the one we found here. This theoretical expectation does indeed appear to match the behavior of the (steep spectrum) Narrow Line Seyfert 1’s, which have a large amount of ionized reflection (NLS1 – Pounds, Done & Osborne 1995; Vaughan et al. 1999). This supports the picture where the difference between NLS1s and normal Seyfert 1s is that NLS1s accrete at a high fraction of the Eddington limit (Pounds et al. 1995), as the steep spectrum gives a low Compton temperature and so reflection from highly ionized as opposed to extremely ionized material. However, this correlation does *not* hold for MCG–6–30–15, which has a steep spectrum together with a large amount of apparently *neutral* reflection (Lee et al 1999; Zdziarski et al 1999), although the variability of the line may indicate that ionization effects are important (Reynolds 2000).

4.3. Multi-radius reflection spectra

Clearly the models used here are incomplete. The optical depth of the ionized layer changes as a function of radius, and relativistic smearing effects should also be included. However, it is clearly necessary to develop a basic understanding of how the complex ionization models differ from simplified single zone ones for a specific radius with no relativistic effects. Having understood that, one can move to the reflected spectra for complete disks, which we plan to do in future work.

Based on physical intuition and some preliminary work, we can speculate on the full disk spectra. NKK and Nayakshin & Kallman (2000) show that if the illuminating X-ray flux, F_x , exceeds that of the locally produced disk thermal emission, F_d , and the X-ray spectrum is relatively hard, i.e., $\Gamma \lesssim 2$, then the skin is nearly completely ionized. The depth of the completely ionized skin decreases with increasing radius in the disk (see Nayakshin 2000a). Hence, larger radii contribute relatively more of the atomic features (e.g., $K\alpha$ line and iron edges) to the overall spectrum, while smaller radii contribute less. If $\tau_h >> 1$ in the inner disk then the extremely relativistic reflected signature will be absent from the data. A low ionization reflection signature is only seen from radii larger than the point at which $\tau_h \sim 1$. This would suppress the broadest components of the iron line, so could make the derived line profile look *qualitatively* like that from a truncated disk (see Fig. 2b in Nayakshin 2000b). One still hopes that detailed and direct spectral fitting, combined with future more sensitive observations, will allow us to discriminate between the physically truncated and completely ionized disks.

4.4. Soft X-ray excess

The key element in the complex ionization models is that for hard X-ray spectra the ionization instability results in a sharp discontinuity between the extremely ionized (invisible) skin and the low ionization material which gives a clearly identifiable reflection signature. Given further complications that can arise due to relativistic broadening in the disk, it is quite likely that the *full* X-ray illuminated disks have a reflected continuum which can mimic that of a truncated disk. Can we then distinguish between these two models? We have shown that there are *observational* tests. Firstly broad bandpass, high signal-to-noise data should show the deficiencies in the `pexrav` model fit (see Figure 3). Such data currently exist only for the Galactic Black Hole Candidates, with Cyg X-1 having the best determined spectrum (Gierlinski et al. 1997; di Salvo et al. 2000). These clearly show that the reflected spectrum from single ionization state material illuminated by a Comptonized continuum is insufficient to describe the observed spectral curvature.

Further, even in the 2–20 keV bandpass there is an observable difference between the single zone and complex ionization reflection models. The complex ionization disks predict the existence of a highly ionized reflected skin which contributes to the spectrum at low energies. Physically, since there is no photo-absorption opacity left in the skin, photons of all energies are scattered (reflected) rather than being absorbed in the skin.

The low ionization reflection component has negligible flux at low photon energies (see, e.g., Basko et al. 1974, Lightman & White 1988), so that spectrum from complex ionization models yields a soft excess as compared with the single-zone models, which can be modeled by a broad spectral component at low energies. An additional and significant source of the soft X-ray excess is the bremsstrahlung emission in the skin, and Compton down-scattered reflected flux. According to the analytical theory of the Compton reflection in the ionized skin (Yakill

et al. 1981; Nayakshin 2000), cooling due to bremsstrahlung emission constitutes between \sim zero (at the top of the skin) and $2/3$ of the total cooling rate (on the bottom). The characteristic temperature at which the Compton-heated branch ceases to exist is of order a few hundred eV to a few keV (see Fig. 1), so that the soft X-ray excess will be rolling over at similar energies, consistent with our results here.

There is a considerable evidence for a similar soft excess in the Galactic Black Hole Candidates. Cyg X-1 plainly shows such a component in ASCA (Ebisawa et al., 1996) and SAX (di Salvo et al., 2000) data, and this is probably the reason why the RXTE results include a blackbody at ~ 1 keV rather than a reflected component (Dove et al 1997). Figure 5a shows the PCA RXTE data of Cyg X-1 (dataset 10241, as used by Dove et al., 1997) fit to a simple single zone ionization model ($\chi^2_\nu = 19.1/38$), while Figure 5b shows the resulting fit including soft component ($\chi^2_\nu = 11.5/35$). The spectrum is much better described with the inclusion of the soft component. The resulting spectral curvature is detected at ≥ 99 per cent confidence on an $F = (\Delta\chi^2/\delta\nu)/\chi^2_\nu = 7.7$ test, and these real data look remarkably like the synthesized model spectra shown in Figure 4.

Clearly this can be interpreted as strong evidence for the existence of complex ionization structure in the accretion disk. However, this is not unambiguous as the GBHC have other ways to produce spectral curvature since the seed photons from the disk are so close to the energy range observed. A truncated disk with hot inner flow produces a Comptonized spectrum where the first few scattering orders are anisotropic, since the illuminating disk photons are anisotropic. This produces a soft excess of about 10 per cent of the isotropic spectrum, i.e. similar in size to that expected from the complex ionization reflected spectrum (P.T. Źycki, private communication). Additionally, the transition between the cool truncated disk and hot inner flow is unlikely to be completely sharp, and there may be a further soft component from heated disk material. These would both affect the GBHC spectra more than those from AGN, so perhaps the true test of whether the disk has complex ionization structure or is truncated is whether the AGN with flat spectra are significantly better fit by including a soft excess component. However, even with the AGN there are ambiguities. One of the most promising models for the origin of the variability behavior of AGN and GBHC has spectral evolution of the Comptonized component from individual flares. This results in a time averaged spectrum which is significantly curved, similar to the curvature seen here in Cyg X-1 (Poutanen & Fabian 1999). We caution that deconvolving the reflected spectrum from more realistic, complex continuum models will have to be done before we can observationally test whether the truncated disk or complex ionization models give a better description of the data.

5. SUMMARY

In this paper, we have shown that reflected X-ray spectra from models which include hydrostatic balance for the illuminated gas have very different properties than single zone ionization models. In the former models, due to the thermal ionization instability, the vertical disk structure is almost discontinuous, with a dramatic transition from an extremely ionized skin on the top to a low-to-moderate ionization material below it. The reflection signature is then a composite of a power law like spectrum from the extremely ionized material, and a low ionization reflection component from the

terial below the skin. The constant density reflection models do not have such a discontinuous behavior. As a result, when the spectra of hydrostatic balance models are fit with simpler, single ionization zone models (Done et al. 1992; Magdziarz & Zdziarski 1995), the physical parameters of the reflector can be miscalculated by a large factor. The single zone models fit to the low-to-moderate reflection component, which is weak even with respect to the incident power law due to scattering in the ionized skin. But the ionized skin reflection cannot be reproduced in the single zone models, so this power law like reflected component is misidentified with the incident power law. Since the reflected fraction Ω is proportional to the ratio of the inferred reflected spectrum to that of the illuminating, then this further dilutes the “observed” reflected fraction.

This implies that the values of $\Omega/2\pi < 1$ often seen in GBHC and AGN may be an artifact of the constant density reflection models used, and need not necessarily mean that the cold SS disk is truncated at some distance $R > 3R_s$. Further, our results also imply that a low value of ionization parameter (and “neutral” line at 6.4 keV), as found by the single zone ionization models, *does not* prove that the material is actually cold. On the contrary, the upper layer of the disk may be completely ionized and obscure the cold material below. These findings are in agreement with earlier suggestions of Nayakshin (1999b) and Ross, Fabian & Young (1999).

In addition, we find an apparent correlation between the power law index Γ of the X-ray continuum and the reflection fraction. This correlation is similar to the one reported by Zdziarski et al., (1999) for AGN and GBHC. We produce the correlation using only the physical nature of the ionization instability for X-ray illuminated gas in hydrostatic balance. This should operate in *all* models where the accretion disk is illuminated by an X-ray source. In particular, other ways to produce the correlation of the amount of reflection with Γ such as a moving inner disk edge (e.g. Poutanen 1998) or with anisotropic illumination by magnetic flares (Beloborodov 1999a,b) will produce even stronger correlations with the inclusion of the ionization physics. The *only* situation where the instability is unimportant for the observed reflected spectrum is if the optical depth of the hot layer is always very much less than unity. However, one clear prediction of the ionization in-

stability is that the steep spectrum AGN should have strongly ionized reflected spectra, which does indeed seem to be the case for the narrow line Seyfert 1 class of AGN (although not for the archetypal extreme relativistic disk object MCG-6-30-15). Thus it seems likely that the ionization instability *is* important in determining the observed reflected spectrum, although it may operate in conjunction with anisotropic illumination or a moving disk edge.

We show that reflection from the ionized skin produces a soft X-ray continuum which can be modeled as a broad soft X-ray excess, similar to that seen in data from Cyg X-1. Taken together, our findings revive models for magnetic flares above an untruncated accretion disk in AGN and GBHCs which seemed to be ruled out by observations of the small solid angle of the reflector (see, e.g., the discussion in Done & Źycki 1999). It seems likely that radial gradients in the ionization structure should be able to suppress the extreme relativistic iron line profile from the inner disk, and so lead to the observed apparent truncation of the disk in the low/hard state GBHC and in some AGN. However, this should be confirmed by further detailed modeling involving complete disk spectra and relativistic smearing.

Finally, another difficulty in unambiguously determining between complex ionization structure on a disk which extends down to the last stable orbit, and a truncated disk, is that the underlying illuminating continuum shape is not well understood. Continuum curvature can mimic the “soft excess” signature of complex ionization structure, and is predicted in the truncated disk geometry, and by models of the variability. Sadly, the observational constraints on the geometry of the accretion flow around the black hole in Cyg X-1 still cannot distinguish between disk/corona and ADAF models for the X-ray emission. On the other hand, new data and complete disk calculations may present better constraints, allowing these very different geometries (and accretion theories) to be distinguished.

6. ACKNOWLEDGEMENTS

SN acknowledges support from NRC Research Associateship. The authors thank Demos Kazanas, Piotr Źycki and Andrei Beloborodov for useful discussions.

REFERENCES

Balbus S.A., Hawley J.F., 1991, *ApJ*, 376, 214
 Basko, M.M., Sunyaev, R.A., & Titarchuk, L.G. 1974, *å*, 31, 249
 Basko M.M., 1978, *ApJ*, 223, 268
 Beloborodov, A.M. 1999a, *ApJ*, 510, L123
 Beloborodov, A.M. 1999b, *MNRAS*, 305, 181
 Dabrowski Y., Fabian A.C., Iwasawa K., Lasenby A.N., Reynolds C.S., 1997, *MNRAS*, 288, 11
 Di Matteo T., 1998, *MNRAS*, 299, 15
 Di Salvo T., Done C., Źycki P.T., Burderi L., Robba N., 2000, *A&A*, submitted.
 Done C., Mulchaey J.S., Mushotzky R.F., Arnaud K.A., 1992, *ApJ*, 395, 275
 Done C., Madejski G.M., Źycki P.T., 2000, *ApJ*, in press.
 Done C., Źycki P.T., 1999, *MNRAS*, 305, 457
 Dove J., Wilms J., Masaick M., Begelman M.C., 1997, *ApJ*, 487, 759
 Ebisawa K., Ueda Y., Inoue H., Tanaka Y., White, N.E. 1996, *ApJ*, 467, 419
 Esin A. A., McClintock J.E., Narayan R., 1997, *ApJ*, 489, 865
 Fabian A.C., Rees M.J., Stella L., & White, N.E. 1989, *MNRAS*, 238, 729
 Field G.B., 1965, *ApJ*, 142, 431
 Field, G.B., & Rogers, R.D. 1993, *ApJ*, 403, 94
 Galeev A.A., Rosner R., Vaiana G.S., 1979, *ApJ*, 229, 318
 George I.M. & Fabian A.C., 1991, *MNRAS*, 249, 352
 Gierlinski M., Zdziarski A. A., Done C., Johnson W. N., Ebisawa K., Ueda Y., Phlips F., 1997, *MNRAS*, 288, 958
 Haardt F., Maraschi L., Ghisellini G., 1994, *ApJ*, 432, 95
 Kallman T.R., White N.E., 1989, *ApJ*, 341, 955
 Ka, Y., Kallman, T.R., 1994, *ApJ*, 421, 273
 Magdziarz P., Zdziarski A.A., 1995, *MNRAS*, 273, 837
 Matt G., Perola G.C., & Piro L. 1991, *A&A*, 247, 25
 Matt G., Fabian A.C., Ross R., 1993a, *MNRAS*, 262, 179
 Matt G., Fabian A.C., Ross R., 1993b, *MNRAS*, 264, 839
 Matt G., Fabian A.C., Ross R., 1996, *MNRAS*, 278, 1111
 Miller K.A., Stone J.M., 2000, *ApJ*, in press
 Morrison R., McCammon D., *ApJ*, 270, 119
 Nandra K., George I.M., Mushotzky R.F., Turner T.J., Yaqoob T., 1999, *ApJ*, 523, 17
 Narayan R., Yi I., 1995, *ApJ*, 444, 231
 Nayakshin, S. 1999a, in “Quasars and Cosmology”, ASP Conference Series, ed. G. Ferland & J. Baldwin, p. 43; astro-ph/9812109
 Nayakshin, S. 1999b, in “Quasars and Cosmology”, ASP Conference Series, ed. G. Ferland & J. Baldwin, p. 87; astro-ph/9812108
 Nayakshin S., & Dove, J.B. 2000, submitted to *ApJ* (astro-ph 9811059).
 Nayakshin, S. 2000a, *ApJ*, 534, 718
 Nayakshin, S. 2000b, *ApJ Letters* accepted (astro-ph/0005603)
 Nayakshin, S., Kazanas, D., & Kallman, T. 2000, *ApJ*, 537, 833
 Nayakshin, S., & Kallman, T. 2000, *ApJ* accepted (astro-ph/0005597).
 Pounds K.A., Done C., Osborne J.P., 1995, *MNRAS*, 277, L5
 Poutanen J., Fabian A.C., 1999, *MNRAS*, 306, L31
 Raymond, J.C. 1993, *ApJ*, 412, 267
 Ross R.R., Fabian A.C., 1993, *MNRAS*, 261, 74.

Ross R.R., Fabian A.C., Brandt W.N., 1996, MNRAS, 278, 1082
Ross R.R., Fabian A.C., Young A.J., 1999, MNRAS, 306, 461
Różańska A., Czerny B., 1996, AcA, 46, 233
Różańska A., 1999, MNRAS, 308, 751
Shakura, N.I., Sunyaev, R.A. 1973, A&A, 24, 337
Smith D.A., Done C., 1996, MNRAS, 280 355
Stern B.E., Poutanen J., Svensson R., Sikora M., Begelman M.C., 1995, ApJ., 449, 13
Sunyaev R.A., Titarchuk L.G., 1980, A&A, 86, 121
Tanaka Y. et al., 1995, Nature, 375, 659
Vaughan S., Reeves J., Warwick R.S., Edelson R., 1999, MNRAS, 309, 113
Zdziarski A.A., Lubinski P., Smith D.A., 1999, MNRAS, 303, 11
Życki P.T., Done C., Smith D.A., 1997, ApJL, 488, 113
Życki P.T., Done C., Smith D.A., 1998, ApJL, 496,25
Życki P.T., Done C., Smith D.A., 1999, MNRAS, 305, 231
Życki P.T., Czerny, B. 1994, MNRAS, 266, 653
Życki P.T., Krolik J.H., Zdziarski A.A., Kallman T.R., 1994, ApJ., 437, 597.

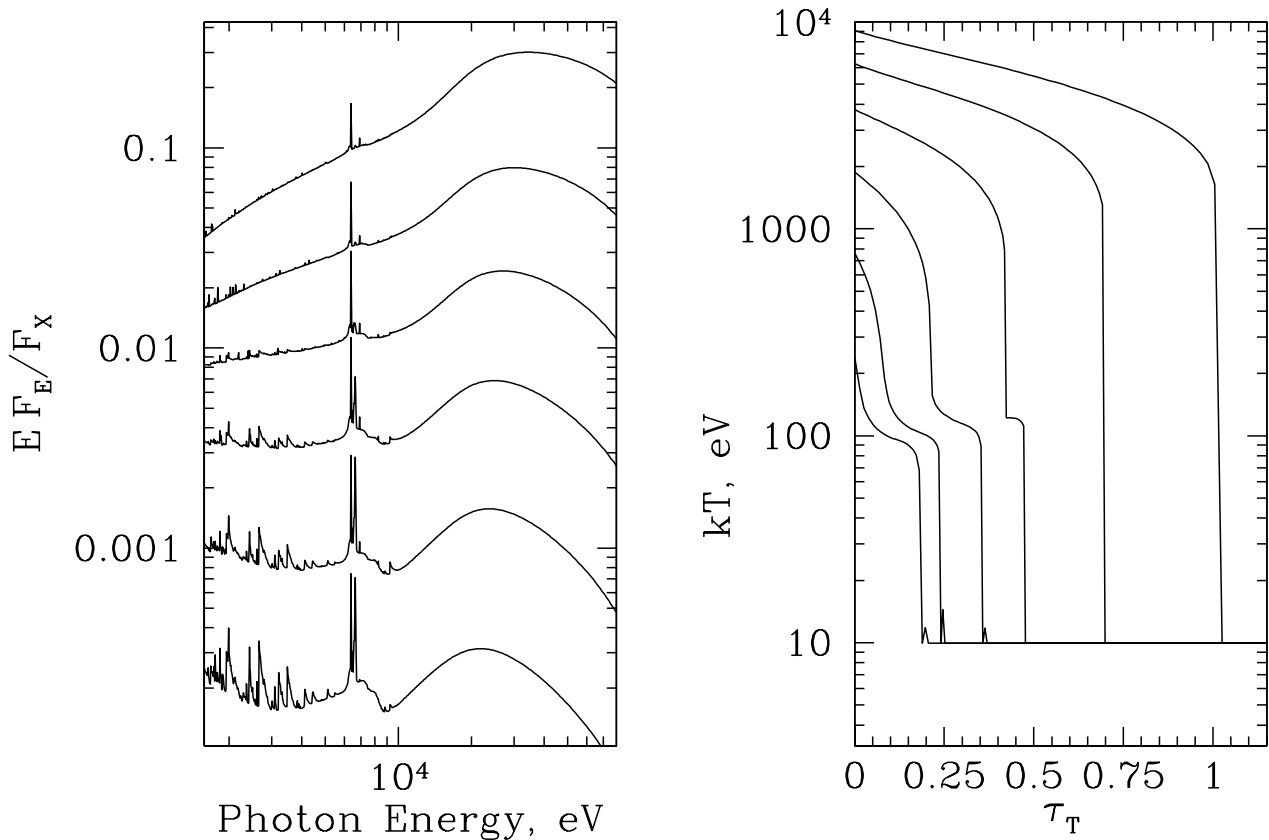


FIG. 1.—Reflected spectra (left) and temperature profiles (right) for 6 different spectral indices ($\Gamma = 1.5, 1.7 \dots 2.5$) calculated with the NKK code for a fixed gravity parameter $A = 0.3$. Note that for harder spectra, the gas temperature is higher and the ionized skin is thicker. This gives the apparent correlation of Γ and $\Omega/2\pi$ shown in Figure 2

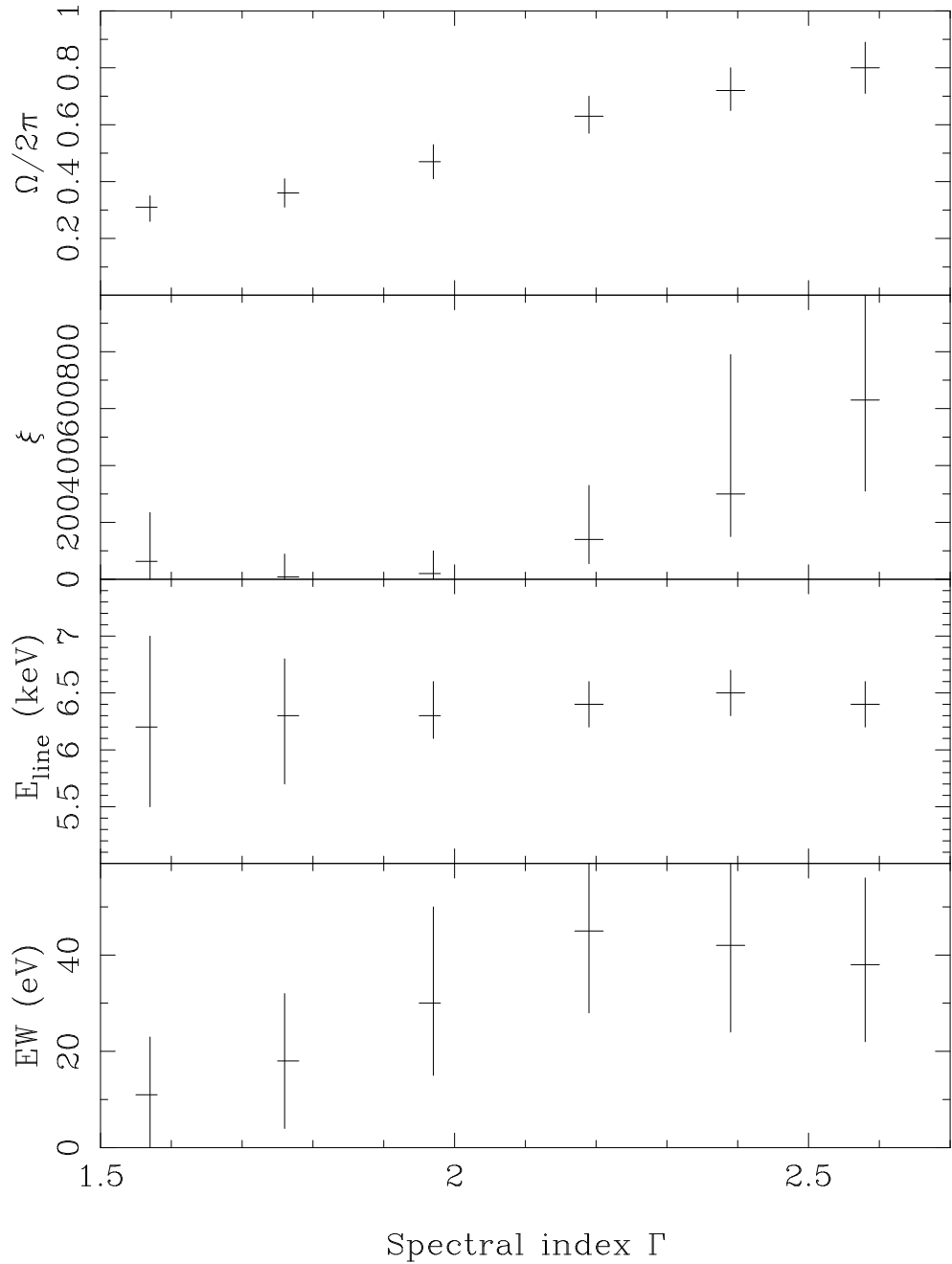


FIG. 2.— The complex ionized disk models of Nayakshin et al. (2000) for $A = 0.3$ as seen in a 10^4 second GINGA exposure are fit to a model of a power law (with exponential cutoff) and a single zone ionized reflection model with separate iron line. The best fit reflected spectral parameters are clearly correlated with the parameters of the illuminating spectrum. The amount of reflection $\Omega/2\pi$ increases with spectral steepness, as does its ionization state. The iron line energy and equivalent width errors are too large to independently constrain the ionization state

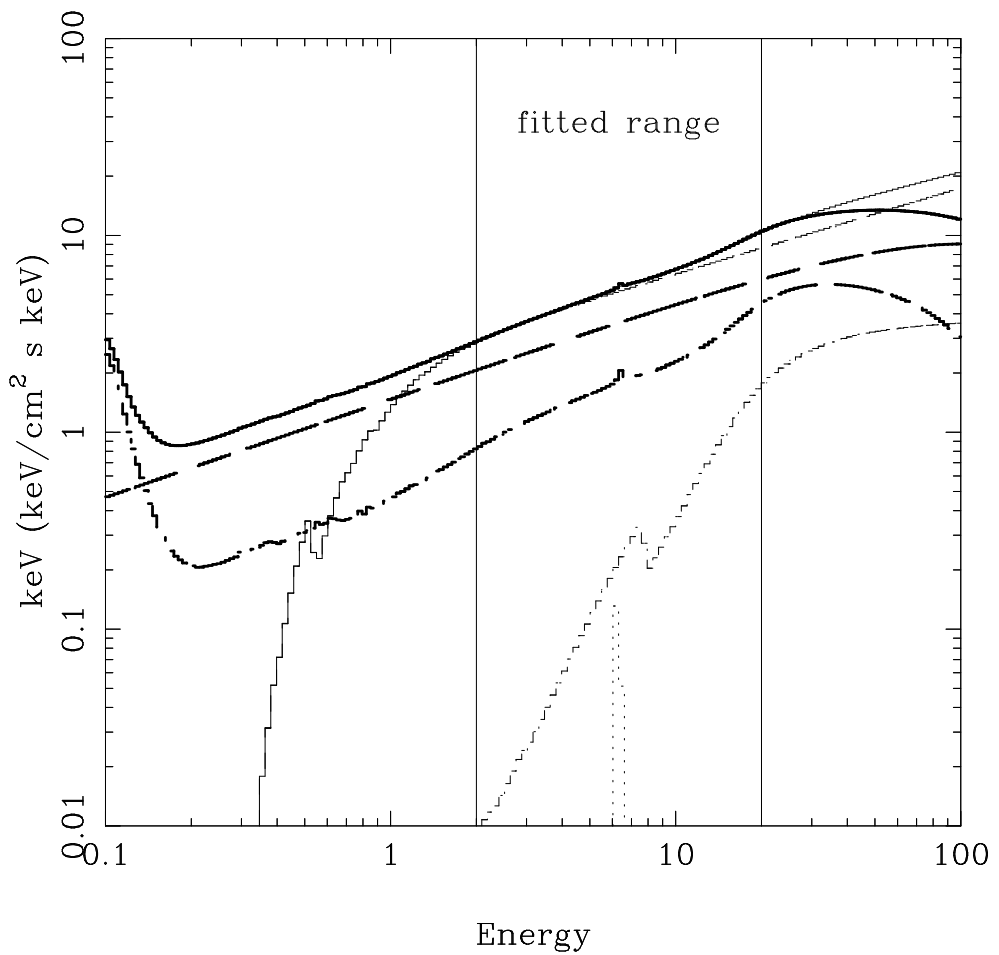


FIG. 3.— The heavy lines show the complex ionization model spectrum for $\Gamma = 1.5$. The long dashed line is the intrinsic illuminating spectrum, while the dash-dot line shows the reflected flux and the solid line is their total. The thin lines show the best fit single zone ionization model components, again with the long dashed line giving the derived illuminating continuum, the dash-dot line giving the reflected continuum. The dotted line is the separate Gaussian line and the solid line is the total spectrum. The best fit single zone ionization reflected continuum dramatically underestimates the true reflected spectrum, but the total spectra over the fitted 2–20 keV range are almost identical

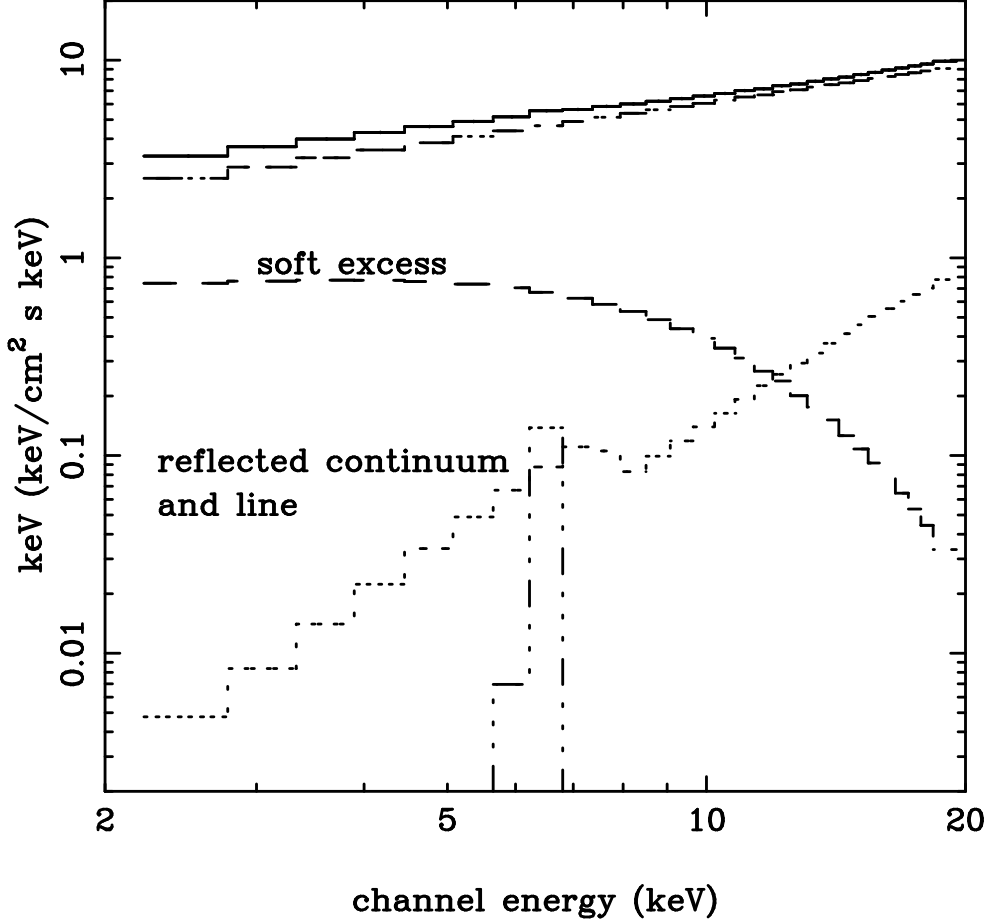


FIG. 4.— The complex ionization model with $\Gamma = 1.5$ fit to the single zone reflector model, together with an additional soft component. The soft component is strongly required by the “data” (compare the fit statistic in Table 1 and Table 2). It is used to model the excess reflected flux at low energies which cannot be matched by the fairly low ionization reflector required by the single zone ionization models to match the iron edge and rise to higher energies.

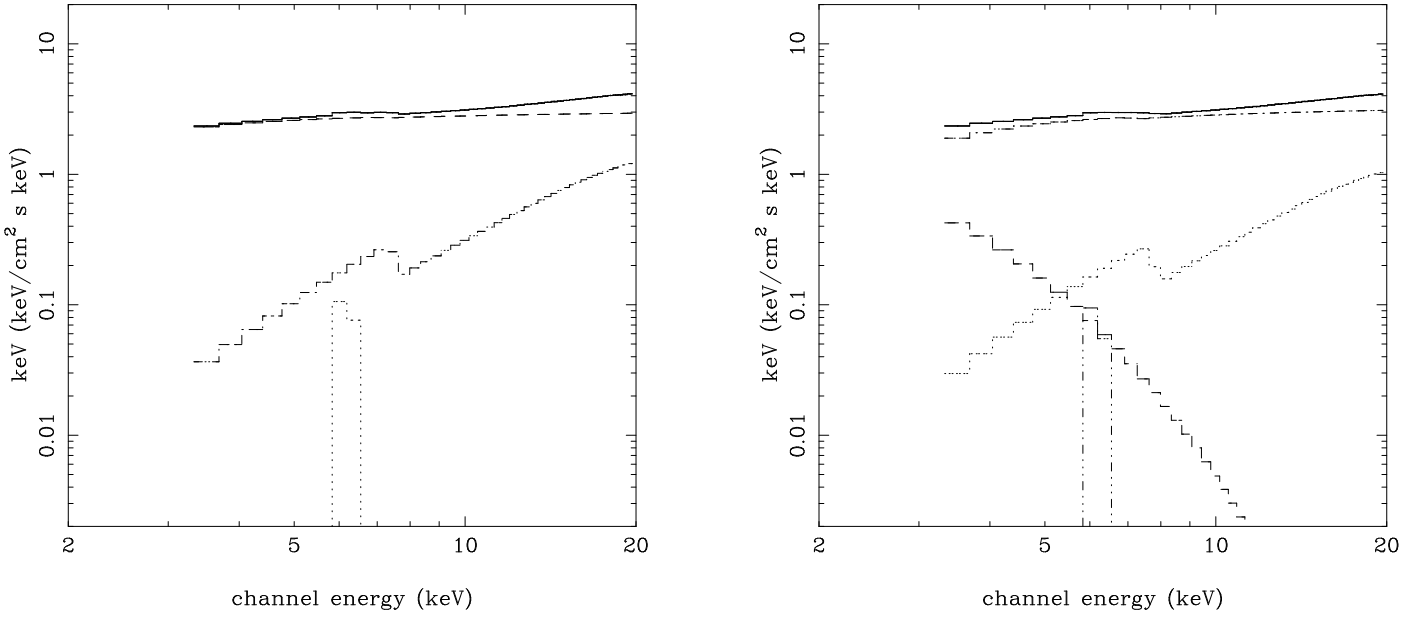


FIG. 5.— The single zone ionization model fit to the *observed* RXTE PCA spectrum of Cyg X-1. This instrument has similar energy resolution to GINGA, and 0.5 per cent systematic errors are included on the top layer data from PCA detectors 0 and 1. Panel (b) shows the fit including a soft component.